Thermal/mechanical properties of short carbon fibre/SiC co-reinforced graphite matrix composites produced by low temperature hot pressing

Yongjun Han[1,2], *Qingzhi Yan*[1], *Xianhui Li*[1]

[1]*Institute of Special Ceramics and Powder Metallurgy, University of Science and Technology Beijing, 30 Xueyuan Road, Haidian District, Beijing 100083, People's Republic of China*
[2]*School of Chemistry and Chemical Engineering, Pingdingshan University, Henan 467000, People's Republic of China*
E-mail: qzyan@ustb.edu.cn

Published in Micro & Nano Letters; Received on 15th January 2015; Accepted on 11th March 2015

Short carbon fibre and silicon carbide (SiC) co-reinforced graphite matrix composites were prepared with natural flaky graphite as raw materials by low temperature hot pressing at 1900°C. The flexural strength in the direction perpendicular to the graphite layers reached 221 MPa for carbon fibre of 5 vol% and SiC of 30 vol%, which was an improvement of 275% compared with pure graphite materials. The composites improved the bend strength of the block obviously, while maintaining the thermal conductivity of 220 W/m K in the direction perpendicular to the hot pressing. The new process has the advantages of being a non-pitch binder process which avoids the high temperature graphitisation operation.

1. Introduction: As one of the most attractive candidates for application as a thermal management device, such as heat exchangers and heatsinks, carbon/graphite possess excellent chemical and physical properties, such as resistance to corrosive environments, high thermal conductivity, low thermal expansion and density [1–3]. However, the common polycrystalline graphite has a very low thermal conductivity of 70–150 W/m K. Moreover, the poor mechanical properties of conventional carbon/graphite materials represent an obstacle for applications where strength is a consideration [4, 5].

To improve the properties of carbon/graphite materials, it is necessary to modify the carbon/graphite matrix by introducing some reinforcement, such as fibres or particles [6]. Zhang *et al.* [7–9] studied the effect of dopants (such as Ti and Si) on the properties and microstructure of graphite. A thermal conductivity up to 285 W/m K was obtained for graphite with 7 wt% titanium, however the bend strength was only 37.4 MPa. Fan *et al.* [10] studied the effects of ball-milling dispersion processes on the properties of fine-grain doped graphite. The sample had a high bending strength (116 MPa) and good thermal conductivity (210 W/m K). However, their study showed excellent thermal properties, but poor mechanic properties of composites, which restricted their use as a thermal management device where high strength was necessary or else, a high temperature (>2500°C) process is inevitable for graphitisation [11].

In the work reported in this Letter, short carbon fibre and silicon carbide (SiC) particle co-reinforced graphite matrix composites were prepared by low temperature hot pressing. The effect of the short carbon fibre on the thermal properties and mechanical properties of composites was analysed in detail.

2. Experimental

2.1. Samples preparation: The natural flaky graphite (NFG) with purity of 99.9% and mean particle size of 10 μm were used as raw materials. The SiC with a mean particle size of 0.5 μm, purity of 98.7% and PAN-short carbon fibre (Csf) were used as reinforcement. Commercially available Al_2O_3 powder (α-Al_2O_3, $d_{50} = 2.02$ μm) and Y_2O_3 powder ($d_{50} = 5$ μm) were used as sintering aids. The matrix materials were 70 vol% graphite and 30 vol% SiC powder with the weight ratio of $SiC:Al_2O_3:Y_2O_3 = 91:6:3$.

The short carbon fibres and matrix materials were ball-milled for 5 h in a polyethylene bottle using ZrO_2 balls and ethanol as the mixing media; the range of the Csf content were 0, 5 and 10 vol % based on densities of 2.26 g/cm^3 for graphite, 1.76 g/cm^3 for Csf, 3.98 g/cm^3 for Al_2O_3, 5.01 g/cm^3 for Y_2O_3 and 3.21 g/cm^3 for SiC, and named GR0, GR5 and GR10, respectively. The resulting slurry was dried and screened through a 200-mesh sieve. Every batch mixture was loaded into a graphite die to be hot-pressed at 1900°C for 30 min and a uniaxial load of 40 MPa, then the load was removed, and the specimens were cooled at ~15°C/min at room temperature.

2.2. Testing methods: The bulk density of the composites was measured using the Archimedes' method. The thermal diffusivities of all specimens ($\Phi 6 \times 1.2$ mm) were determined using a laser-flash diffusivity instrument (LFA-457). The morphology of the dispersed powders and the microstructures of the fracture surface and polished surfaces were observed via scanning electron microscopy (SEM). The phase assemblage was identified by X-ray diffraction (XRD).

3. Results and discussion

3.1. Phase composition and microstructure: To assess the effect of Csf and SiC on the orientation of the NFG obtained by the hot-pressing process, XRD measurements of raw NFG powders, SiC powders and SiC/graphite composites with 5 and 10 vol% Csf were performed. There was one sharp reflection at $2\theta = 26.5°$ which is attributed to THE (002) crystal plane of the hexagonal graphite and other weak peaks corresponding to the (004), (100), (101), (110) and (112) crystal planes in the XRD pattern of the raw NFGs powders can be clearly observed in Fig. 1*a*. Figs. 1*c* and *e* show the XRD patterns of the samples with 5 and 10 vol% Csf perpendicular to the hot-pressing direction. The (002) and (004) diffraction peaks can be observed, and the intensity of these two peaks from the graphite is greater than that of NFGs powders. The (100), (101), (110) and (112) diffraction peaks disappear. From the patterns parallel to the hot-pressing direction series (Figs. 1*d* and *f*), the intensity of the plane (100), (101), (100) and (112) increases at the same peak position. The highly directional orientation of the NFGs during the hot-pressing process is attributed to the prominent changes [12, 13]. The α-SiC diffraction peaks which are present in the XRD pattern of the raw SiC powders (Fig. 1*b*) can also be observed in Figs. 1*c–f*. The sharp increase in the intensity of the SiC peaks relative to the

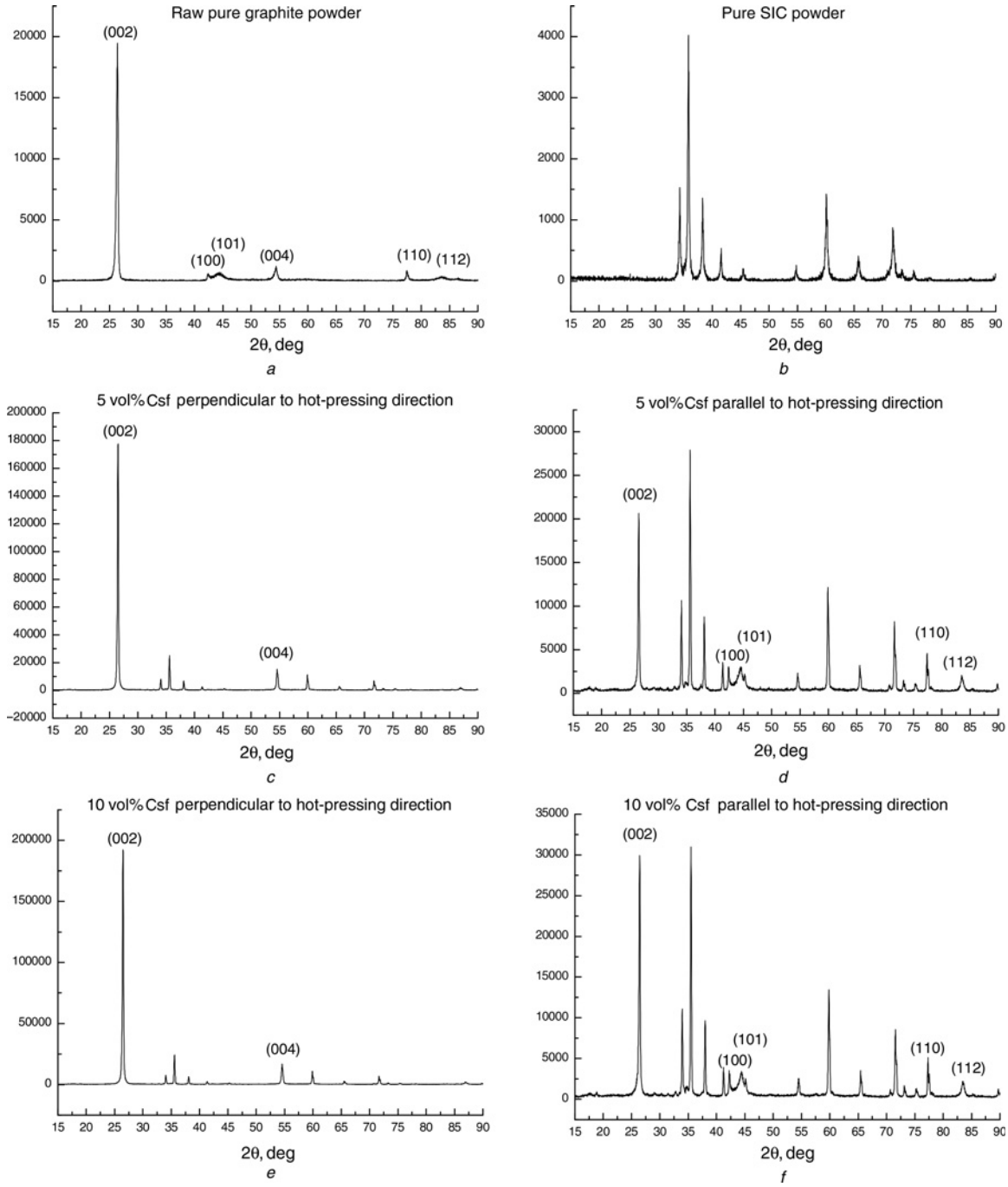

Figure 1 *XRD spectrum of the raw graphite, SiC and composites*

(002) diffraction peak for graphite further demonstrates that the NGFs have been well aligned with the hot pressing. The relative intensity of the (002) diffraction peak, compared to the corresponding (110) diffraction peak and diffraction SiC peaks in Fig. 1*d* is higher than that of Fig. 1*f*. This reflects the decreased orientation of the NGFs with the increase of the Csf fraction.

The SEM micrograph taken from the surface perpendicular to the polished hot-pressing surface of the composites in Fig. 2 shows a continuous graphite matrix and uniformly dispersed SiC and Csf. The planar flakes of NFGs were oriented in the direction perpendicular to hot pressing. The fibres were distributed along the graphite layers of the NFGs randomly. The two-dimensional (2D) structure was developed because of the rotation under the pressing leading to a favourable orientation of the Csf and NFGs, the reinforced mode was 2D reinforcement. Csf in composites after sintering at 1900°C presented apparent scaly spalling as shown in Figs. 2*b* and 3*b*. This was because of the transformation from an amorphous state to the 3D ordered graphite structure for Csf in the sintering process. An induced graphitisation region was developed around the surface of Csf, where the growth of the graphitic crystallites was parallel to the fibre axis, while the shrinkage of the graphite matrix would produce squeezing and friction on the Csf, resulting in a distinct morphology damage.

3.2. Mechanical properties and thermal properties of the composites: The properties of the composites are listed in Table 1. It can be seen that compared with GR0, the body density decreases with Csf fraction. The decreased densities were attributed to the addition of Csf with a lower density than SiC and graphite. The bend strength reached 221 MPa for the Csf

doi: 10.1049/mnl.2015.0004

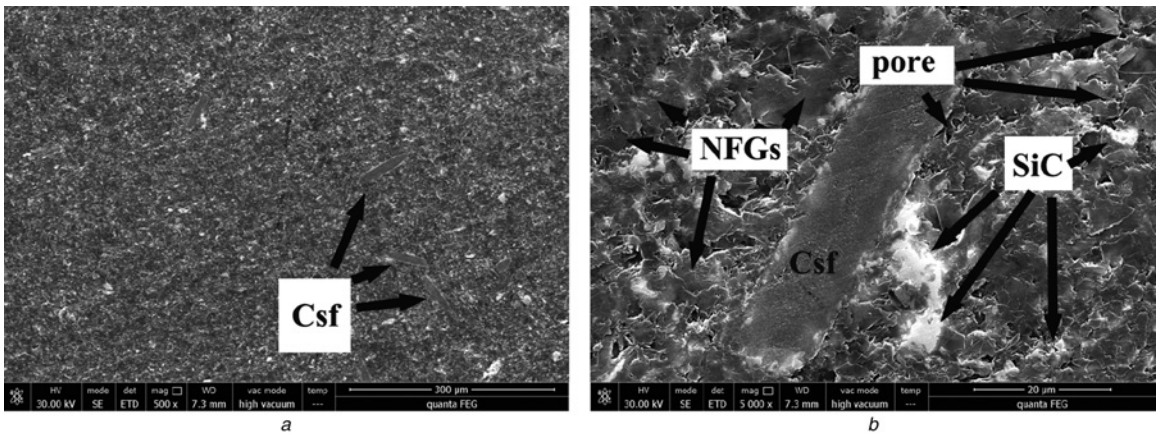

Figure 2 *SEM images of GR5 perpendicular to the hot-pressing direction*

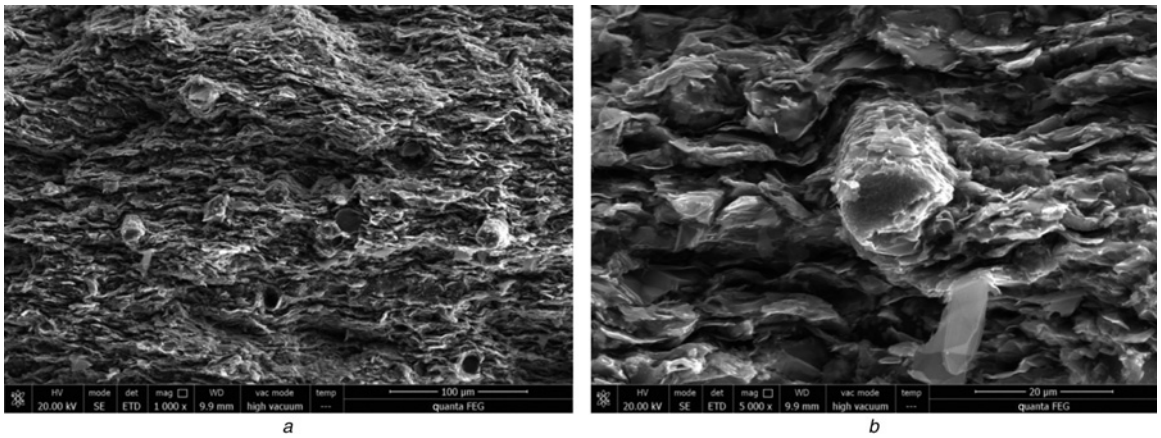

Figure 3 *SEM fracture image of the GR5 composites*

content of 5 vol%, which was 1.67 times that of GR0 and 3.7 times that of the commercial high-strength graphite block. This implied a distinct strengthening effect for the graphite matrix co-reinforced by SiC particles and Csf. The possible mechanism for reinforcement was the pullout effect of Csf and the dispersion strengthening effect of the SiC particles in the graphite matrix, which hindered the fracture of the graphite layers when under load. However, the bend strength decreased with the Csf fraction reaching 10 vol% because of the increasing number of pores caused by the fibre bridging effect. The pores weaken the bond strength of the fibre/matrix interface, and then weaken the mechanical property of composites.

The SEM images of the fractured surface of sintered materials (Fig. 3) show that the composites possess a lamellar compacted structure with low porosity. The homogeneous distribution of the equiaxed SiC particles was in favour of load transformation, which could effectively increase the flexural strength and fracture toughness of the composites. The pullout of Csf and their residual holes is obvious in Fig. 3*a*, and the Csf grown surface was rough after hot pressing, as shown in Fig. 3*b*. This indicates the appropriate association among Csf, SiC particles and the graphite matrix.

The thermal conductivity in the perpendicular direction to the hot-pressing direction with 5 vol% Csf was ~220 W/m K, which was two times that of common polycrystalline graphite. The slight decrease with Csf fraction could be because of the decreased orientation of the NFGs during the hot pressing and the heat resistance of the interface among Csf, SiC and the graphite matrix. The porosity of GR10 increased slightly, resulting in more defects, and reduced the continuity of the thermal transport link. That is why the in-plane thermal conductivity of GR10 was lower than that of GR5. The thermal conductivity in the parallel direction was much lower than the in-plane thermal conductivity for all samples because of the preferred orientation of the graphite flake and Csf along the perpendicular to the hot-pressing direction.

Table 1 Thermal and mechanical properties of composites

Materials	Csf fraction, %	Density, g/cm^3	Porosity, %	Bending strength, MPa	T_c, W/m·K, ⊥/‖
GR0	0	2.42	5.46	132	200/30
GR5	5	2.35	5.88	221	220/35
GR10	10	2.27	7.65	140	180/32

4. Conclusion: Csf and SiC co-reinforced graphite matrix composite was prepared by the hot-pressing process without the pitch-binder which avoids the high temperature graphitisation operation. It was found that the mechanical properties of the composites were improved obviously while maintaining the excellent in-plane thermal conductivity. The increase of mechanical properties was mainly ascribed to the pullout of fibres and the dispersion strengthening effect of the SiC particles in the graphite matrix. It is suggested that the introduction of Csf and SiC into the graphite matrix is a potential approach to enhance the mechanical properties of graphite with excellent thermal conductivity.

5. Acknowledgments: Financial support from the Natural Science Foundation of China under Contract No. U1134102 is gratefully acknowledged.

6 References

[1] Wang Y.-G., Korai Y., Mochida I.: 'Carbon disc of high density and strength prepared from synthetic pitch-derived mesocarbon microbeads', *Carbon*, 1999, **37**, pp. 1049–1057

[2] Yamamoto O., Imai K., Sasamoto T., Inagaki M.: 'Preparation of carbon material with SiC-concentration gradient by silicon impregnation and its oxidation behaviour', *J. Eur. Ceram. Soc.*, 1993, **12**, pp. 435–440

[3] Tricot G., Nicolaus N., Diss P., Montagne L.: 'Inhibition of the catalytic oxidation of carbon/carbon composite materials by an aluminophosphate coating', *Carbon*, 2012, **50**, pp. 3440–3445

[4] Pierson H.O.: 'Handbook of carbon, graphite, diamonds and fullerenes: processing, properties and applications' (William Andrew, Norwich, NY, 1994)

[5] Wen C.-Y., Huang G.-W.: 'Application of a thermally conductive pyrolytic graphite sheet to thermal management of a PEM fuel cell', *J. Power Sources*, 2008, **178**, pp. 132–140

[6] Manocha L.M., Yasuda E., Tanabe Y., Kimura S.: 'Effect of carbon fiber surface-treatment on mechanical properties of C/C composites', *Carbon*, 1988, **26**, pp. 333–337

[7] Qiu H., Han L., Liu L.: 'Properties and microstructure of graphitised ZrC/C or SiC/C composites', *Carbon*, 2005, **43**, pp. 1021–1025

[8] Garcıa-Rosales C., Ordas N., Oyarzabal E., *ET AL.*: 'Improvement of the thermo-mechanical properties of fine grain graphite by doping with different carbides', *J. Nuclear Mater.*, 2002, **307**, pp. 1282–1288

[9] Franzen P., Haasz A., Davis J.: 'Radiation-enhanced sublimation of doped graphites', *J. Nuclear Mater.*, 1995, **226**, pp. 15–26

[10] Fan Z., Liu L., Li J., *ET AL.*: 'The preparation of fine-grain doped graphite and its properties', *J. Nuclear Mater.*, 2002, **305**, pp. 77–82

[11] Liu Z.J., Guo Q.G., Song J.R., Liu L.: 'Effect of Ti dopant on shrinkage and performance of MCMB-derived carbon laminations', *Carbon*, 2007, **45**, pp. 146–151

[12] Yuan G., Li X., Dong Z., *ET AL.*: 'Graphite blocks with preferred orientation and high thermal conductivity', *Carbon*, 2012, **50**, pp. 175–182

[13] Zhao Y., Shi J., Wang H., *ET AL.*: 'A sandwich structure graphite block with excellent thermal and mechanical properties reinforced by in-situ grown carbon nanotubes', *Carbon*, 2013, **51**, pp. 427–430

doi: 10.1049/mnl.2015.0004